Dynamic Structural Evolution of Ceria-Supported Pt Particles: A Thorough Spectroscopic Study

Junjun Wang, Eric Sauter, Alexei Nefedov, Stefan Heißler, Florian Maurer, Maria Casapu, Jan-Dierk Grunwaldt, Yuemin Wang,* and Christof Wöll*

ABSTRACT: CeO_2 supported Pt nanoparticles are of prominent technological interest due to their excellent dispersion and thus performance in a wide range of catalytic reactions. In this study, the dynamic structural evolution of Pt supported on ceria particles in response to changes of reaction conditions has been studied by surface ligand infrared spectroscopy in conjunction with X ray photoelectron spectroscopy. The combined results obtained under oxidative and reductive conditions reveal that oxidation at elevated temperatures leads to a pronounced fragmentation of the Pt nanoparticles, yielding positively charged Pt single atoms bound to the surface of the ceria particles. Subsequent reduction carried out at different temperatures leads to the formation of various metallic Pt species including small clusters and nanoparticles, dependent on the dispersion of Pt during the oxidation step and the kind of reduction. The present spectroscopic data provide a thorough insight into the structural and electronic properties of CeO_2 supported Pt particles that show strong changes of charge state and size depending on the reaction conditions.

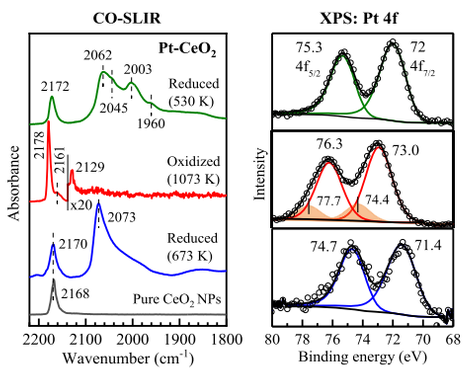

1. INTRODUCTION

Among the metal/oxide catalysts, ceria supported platinum is of particular interest due to its unique catalytic properties and wide range of applications in numerous chemical reactions, including water−gas shift reaction,[1−4] CO oxidation,[5−8] selective hydrogenation,[9−12] gas sensing,[13] automotive exhaust gas cleaning,[14] and production of synthesis gas.[15] Pt/CeO_2 based catalysts are among the most promising candidates to achieve high conversion of pollutants in exhaust emissions at low temperatures.[16] However, Pt is very expensive due to its low natural abundance in the earth's crust that amounts to only about 5 parts per billion by weight. To reduce the cost of the catalysts, it is required to increase the surface area to volume ratio of Pt in catalysts, which maximizes their utilization efficiency. When reducing the size of the particles of this precious metal, it has to be considered, however, that remarkable changes in the electronic structure of metal particles occur.[17−21] For this reason, the effects of decreasing the particle size of Pt, a promising approach to enhance the low temperature activity and selectivity of the catalytic materials, have to be carefully investigated.

Recently, Gänzler et al.[16] developed a protocol that enabled them to tune the size of Pt nanoparticles (NPs) in situ at moderate temperatures. They reported a dynamic structural behavior of Pt NPs deposited on ceria surfaces at temperatures below 500 °C during a cycle of oxidizing/reducing treatments. In an oxidizing atmosphere, redispersion of Pt on CeO_2 occurred. In the subsequent reducing pulses, a controlled formation of Pt particles was achieved. This approach is supposed to be promising for tuning the dispersion and electronic properties of noble metals during operation, with tremendous effects on the low temperature activity of such catalysts.[22−25] Thus, a fundamental understanding of the structural evolution of Pt/CeO_2 catalysts under these oxidation/reduction conditions is of critical importance.

In this study, various Pt species (single atoms, small clusters, and NPs) supported on ceria NPs were characterized by CO surface ligand infrared (CO SLIR) spectroscopy under ultra high vacuum (UHV) conditions using a sophisticated UHV apparatus.[26] This surface sensitive and non destructive ap proach is well suited to characterize the structural evolution of the surface and chemical properties of metal/oxide cata lysts.[27−29] The systematic study using CO SLIR, together with X ray photoelectron spectroscopy (XPS), enabled us to gain detailed insights into the strong Pt−ceria interaction and the dynamic structural evolution of Pt species under oxidative and reductive conditions at different temperatures.

2. EXPERIMENTAL SECTION

Commercial CeO_2 NPs with a surface area of 28 m^2/g were doped with Pt (0.94 wt %) by robot controlled incipient wetness impregnation (accelerator SLT106 Parallel Synthesizer, SLT CATIMPREG, ChemSpeed Technologies).[30] The Pt/CeO_2 catalyst (25 m^2/g after hydrothermal aging), denoted as oxidized Pt/CeO_2, was first calcined in 20% O_2/N_2 at 773 K for 5 h (after this step, referred to as the calcined sample) and then hydrothermally treated at 1073 K for 16 h under 10% O_2 and 10% H_2O in N_2. The oxidized sample was subsequently reduced in 2% H_2/N_2 for 30 min at 673 K to generate reduced Pt NPs, denoted as reduced Pt/CeO_2 (673 K). The detailed sample preparation procedure was described elsewhere.[25] For comparison, the oxidized Pt/CeO_2 NPs were reduced by atomic hydrogen ($p = 5 \times 10^{-5}$ mbar) at lower temperatures (530 K) for 60 min. Exposure to atomic hydrogen was conducted by dissociating H_2 on a hot tungsten filament situated in line of sight from the sample.

The CO SLIR measurements were conducted with an advanced UHV system that combines a state of the art Fourier transform infrared (FTIR) spectrometer (Bruker Vertex 80v) and a multichamber UHV system (Prevac).[27,31] Pt/CeO_2 powders were pressed into a stainless steel grid (about 13 mm in diameter) under the pressure of 5 bar for 2 min with a hydraulic press and then mounted on a sample holder, which was specially designed for the FTIR transmission measurements under UHV conditions. The base pressure in the chamber for infrared (IR) measurements was below 3×10^{-10} mbar. The exposure of the sample to CO was carried out by backfilling the IR chamber up to 0.01 mbar using a leak valve based directional doser connected to a tube (2 mm in diameter) that terminated 3 cm from the sample surface and 50 cm from the hot cathode ionization gauge. The infrared data were accumulated by recording 1024 scans with a resolution of 4 cm^{-1}.

XPS measurements were carried out in a UHV setup equipped with a high resolution RG Scienta 4000 analyzer. Al Kα (1486.6 eV) radiation was used as the excitation source. The energy resolution was better than 1 eV with a pass energy of 200 eV. The binding energies were calibrated based on the C 1s line at 284.8 eV as a reference. The XPS spectra were deconvoluted using software Casa XPS with a Gaussian–Lorentzian mix function and a Doniach–Sunjic function for metallic Pt^0 species.[32]

3. RESULTS AND DISCUSSION

3.1. Structural Evolution of Pt/CeO_2 Nanoparticles Characterized by XPS. We focus first on the XPS investigations of various Pt/CeO_2 NPs pretreated under activation conditions including a consecutive treatment of oxidation and reduction with hydrogen at different temperatures, as described in Section 2. Figure 1 shows the corresponding deconvoluted Pt 4f XPS data. The deconvolution of Pt 4f peaks of reduced Pt/CeO_2, pretreated with H_2 at 673 K, results in a $4f_{7/2}/4f_{5/2}$ spin–orbit doublet at 71.4/74.7 eV, which is the characteristic for metallic Pt^0 NPs.[7,33−37] After the oxidation treatment at 1073 K, two new Pt 4f doublets are clearly resolved. The predominant doublet at 73.0/76.3 eV is ascribed to Pt^{2+} species, while the minority one at 74.4/77.7 eV originates from Pt^{4+} species, in line with the literature data.[33−38] Furthermore, there is no indication of metallic Pt^0, revealing that all Pt atoms were oxidized to Pt^{2+} and Pt^{4+} cations under hydrothermal conditions (10% H_2O, 10% O_2, 1073 K). We note that the electronic and chemical properties of small Pt clusters and NPs differ substantially from those of bulk Pt.

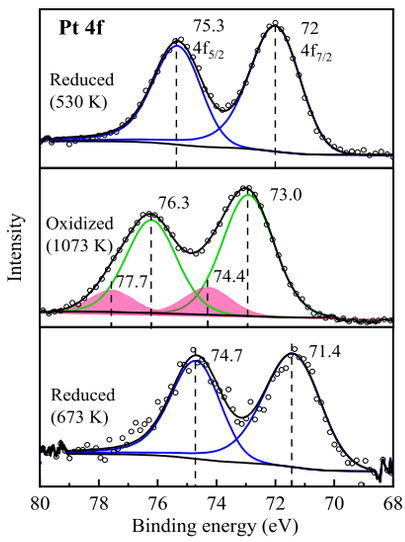

Figure 1. Pt 4f XPS data of reduced Pt/CeO_2 (673 K, bottom), oxidized Pt/CeO_2 (1073 K, middle), adapted with permission from ref 25. Copyright 2020 Springer Nature, and Pt/CeO_2 obtained after reduction of the oxidized sample with H atoms at 530 K (top).

Upon further treatment of the oxidized sample with H atoms at lower temperatures (530 K), the Pt $4f_{7/2}/4f_{5/2}$ peaks shift again to lower binding energies (Figure 1), indicating dynamic changes in the Pt components from positively charged to neutral species. Interestingly, the binding energy of the Pt 4f doublet at 72.0/75.3 eV is slightly higher by 0.6 eV compared with those observed for reduced Pt/CeO_2 pretreated with hydrogen at higher temperatures (673 K). We assign the doublet at 72.0/75.3 eV to the formation of very small Pt^0 clusters, in excellent agreement with those (72.0/75.2 eV) reported for ∼0.08 ML Pt deposited on a $CeO_2(111)$ thin film grown on the Cu(111) substrate.[20] In general, the higher binding energy indicates strong electronic interactions between small Pt clusters and ceria support, leading to charge transfer from Pt to CeO_2. The presence of small Pt clusters is further supported by the CO SLIR spectra, as shown below. We note that the binding energy shift is also related to the Pt particle size. Overall, these XPS results reveal that the CeO_2 supported Pt species significantly change under alternating reductive and oxidative atmospheres at different temperatures.

Figure 2 shows the deconvoluted XPS data of Ce 3d and O 1s for Pt/CeO_2 after the treatments described above. In the Ce 3d spectra (Figure 2a), five $3d_{5/2}/3d_{3/2}$ spin–orbit doublets are resolved and labeled following the convention proposed by Burroughs et al.[39] The v/u, v''/u'', and v'''/u''' peaks are characteristic for Ce^{4+} species, while the v_0/u_0 and v'/u' doublets are attributed to the Ce^{3+} final state. On the basis of a quantitative analysis of the Ce 3d XPS data, the Ce^{3+} content is estimated to amount to 35% for the reduced Pt/CeO_2 (673 K) and 30% for the sample treated with H atoms at 530 K. It should be noted that the shape of the Ce 3d XPS spectrum recorded for the oxidized Pt/CeO_2 (1073 K) is substantially different from those obtained for pure ceria samples.[40] Importantly, after oxidizing treatment at 1073 K, the surface Ce^{3+} concentration is still as high as 18% (Figure 2b). The

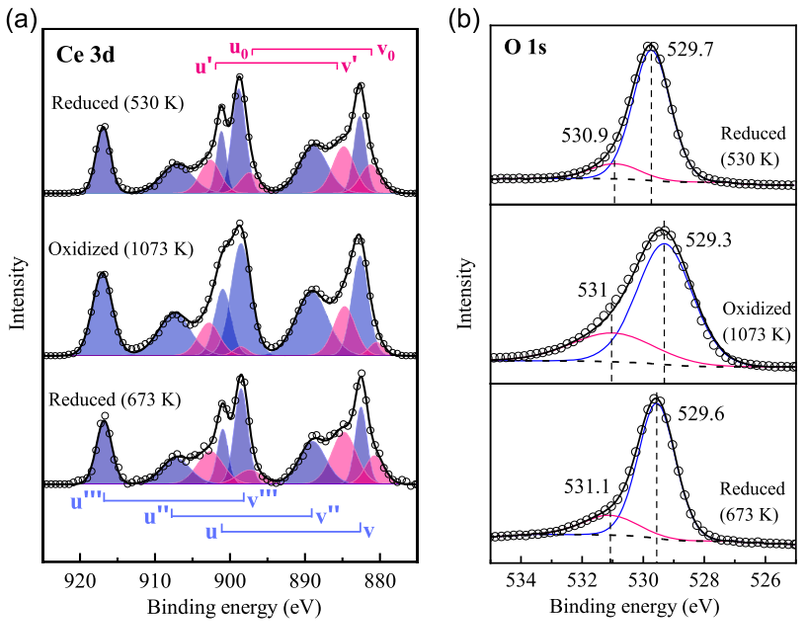

Figure 2. (a) Ce 3d and (b) O 1s XPS data of reduced Pt/CeO_2 (673 K, bottom), oxidized Pt/CeO_2 (1073 K, middle), and Pt/CeO_2 obtained after reduction of the oxidized sample with H atoms at 530 K (top).

observation of high population of Ce^{3+} species indicates a substantial modification in structural and electronic properties of ceria surfaces induced by Pt substitution, as will be discussed later.

The strong interaction between Pt and the ceria surface is further evidenced by the corresponding O 1s XPS spectra (Figure 2b). An intense peak at ~529.6 eV and a weak signal at ~531.0 eV were observed, which are assigned to lattice oxygen anions in the regular CeO_2 coordination[40−42] and oxygen anions located near defect sites, respectively.[40,43−45] Compared to the regular O^{2-} ions, the binding energy of the defect related O 1s core level increases by about 1 eV. This is attributed to the modification of the chemical coordination environment of oxygen anions when coordinated to reduced Ce^{3+}. Importantly, for the oxidized sample (1073 K), the defect related O 1s peak does not disappear but becomes more pronounced (26%). Furthermore, the lattice O^{2-} peak shifts slightly to lower binding energies (529.3 eV, Figure 2b). These findings reveal significant electronic interactions between the Pt and ceria support. On the basis of the XPS data and previous investigations,[25] we propose that Pt was completely oxidized at 1073 K and highly dispersed on CeO_2 surfaces as single atoms, accompanied by surface restructuring of the oxide particles. This migration of Pt into CeO_2 changes the chemical environment of oxygen in the sample, thus explaining the shift of the O 1s peak mentioned above. This assignment is validated by the CO SLIR investigations discussed below.

3.2. CO-SLIR Characterization. The dynamic structural evolution of ceria supported Pt species under different activation conditions is further monitored by SLIR spectroscopy using CO as a probe molecule. Figure 3 shows the corresponding CO SLIR spectra. For the reduced Pt/CeO_2 sample, the IR band at 2170 cm^{-1} is assigned to CO bound to Ce^{3+} defect sites, in line with the observation for CeO_2(111) single crystal surfaces.[40] Furthermore, the spectrum of the reduced Pt/CeO_2 is dominated by an intense IR band at 2073 cm^{-1}, which is assigned to CO bound to highly coordinated Pt atoms exposed by Pt NPs.[46−49] This result demonstrates the

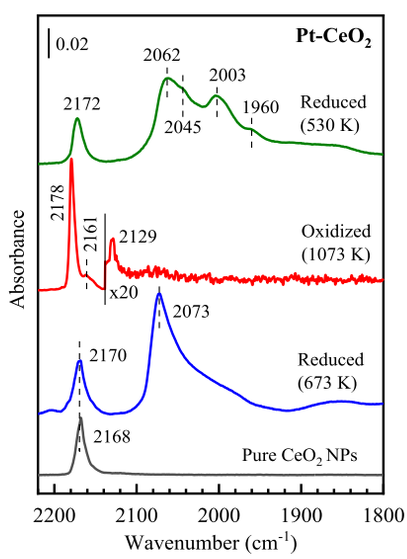

Figure 3. CO SLIR spectra of pure CeO_2 NPs and differently treated Pt/CeO_2 NPs: reduced Pt/CeO_2 at 673 K, oxidized Pt/CeO_2 at 1073 K (adapted with permission from ref 25. Copyright 2020 Springer Nature), and Pt/CeO_2 obtained after reduction of the oxidized sample with H atoms at 530 K. All spectra were recorded in 0.01 mbar CO at 113 K.

formation of metallic Pt NPs as majority species upon reduction with hydrogen at elevated temperatures (673 K), in good agreement with the XPS observation. The presence of Pt NPs is further confirmed by high angle annular dark field imaging scanning transmission electron microscopy (STEM) images (Figure S1) that show an average particle size of 1.1 nm. This value is also in line with that (1.0−1.2 nm) determined by X ray absorption fine structure analysis.[25]

For the oxidized Pt/CeO_2 (1073 K), the metallic Pt^0 related CO vibrations disappear completely, whereas pronounced changes are observed for the CeO_2 related CO bands regarding both frequency and intensity. As shown in Figure 3, a weak IR

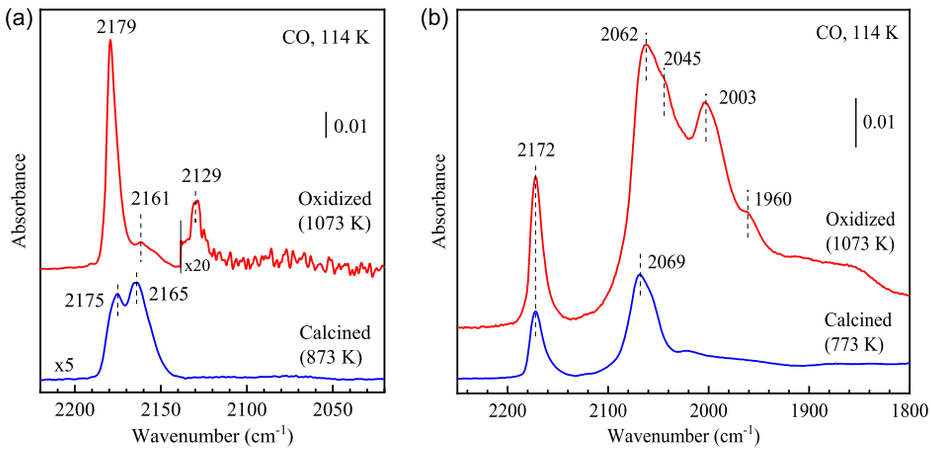

Figure 4. CO SLIR spectra of (a) calcined (773 K) and oxidized (1073 K) Pt/CeO_2 samples and (b) subsequent reduction with H atoms at 530 K. All spectra were recorded in 0.01 mbar CO at 114 K.

band is clearly resolved at 2129 cm^{-1}, which is the characteristic for CO bound to oxidized Pt^{2+} atop species.[50] This assignment is confirmed by recent theoretical work,[25] in which the isolated Pt single atoms are stabilized as Pt^{2+} substitutes at four fold hollow sites by adopting a square planar geometry involving Pt−O−Ce bonds. The computed CO vibrational frequency (2128 cm^{-1}) is in excellent agreement with the IR observation.

The atomic dispersion of Pt NPs and Pt induced restructuring of ceria surfaces are further supported by the significant splitting of the Ce related CO band at 2170 cm^{-1} into two peaks at 2179 and 2161 cm^{-1} after oxidation at 1073 K (see Figure 3). According to the density functional theory calculations,[25] the predominant blue shifted vibration at 2178 cm^{-1} is attributed to CO adsorbed on the surface Ce ions located in the direct vicinity of Pt, whereas the low lying IR band at 2161 cm^{-1} is assigned to CO bound to the surface Ce sites, where the chemical environment is slightly modified due to the restructuring of CeO_2 surfaces induced by Pt substitution in CeO_2. Again, these assignments have been confirmed by computed vibrational frequencies.[25] Since CO can adsorb only at sites exposed at the particle surfaces, these SLIR results demonstrate the presence of highly dispersed Pt single ions on the surface of ceria. This finding is supported by STEM observations (Figure S1), in which no Pt particles were found.[25]

When subjecting the oxidized Pt/CeO_2 sample to a controlled reduction treatment by exposing to H atoms at lower temperatures (530 K), a substantial change is observed in the IR spectrum (see Figure 3). Besides the absorption band at 2172 cm^{-1} assigned to CO bound to Ce cations, intense low lying CO bands appear in the range between 1850 and 2062 cm^{-1}. The Pt NP related IR band at 2073 cm^{-1}, clearly present for the Pt/CeO_2 sample exposed to H atoms at higher temperatures (673 K), is absent after the low temperature H atom exposure. Instead, numerous new CO vibrations at 2062, 2045, 2003, and 1960 cm^{-1} are detected. The bands at 2062, 2045, and 2003 cm^{-1} are attributed to CO adsorbed at different types of under coordinated Pt atop sites present on the surfaces of small Pt clusters,[18,51,52] whereas the 1960 cm^{-1} band can be assigned to CO bound to the Pt (small clusters)−ceria interface in a bridging configuration, in accordance with previous work.[51] Overall, the presented CO SLIR data provide solid evidence that the structural and electronic properties of Pt supported on CeO_2 vary strongly depending on activation conditions.

We have further studied the impact of oxidation conditions on the dispersion of Pt. Figure 4a shows the CO SLIR spectra of Pt/CeO_2 catalysts oxidized at different temperatures (773 and 1073 K). After oxidizing treatments, Pt is well dispersed as Pt^{2+} cations (2129 cm^{-1}) on CeO_2, whereas no IR bands are observed for CO bound to metallic Pt sites. We note that for Pt/CeO_2 oxidized at 773 K, the 2129 cm^{-1} band is not visible, which could be due to the much lower concentration of surface Pt^{2+} single sites compared to the sample oxidized at higher temperatures (1073 K). The corresponding XPS results of Pt 4f, Ce 3d, and O 1s peaks are shown in Figures S2−S4, respectively. The Pt 4f XPS data reveal that all metallic Pt atoms were oxidized to Pt^{2+} and Pt^{4+} cations (Figure S2). As discussed above, the splitting of the CeO_2 related CO vibrations is indicative of strong electronic interactions between Pt and the support, leading to substantial restructur ing of the ceria surface via Pt substitution. Accordingly, the bands at 2175 and 2165 cm^{-1} are assigned to CO bound to surface Ce sites with and without Pt neighbors, respectively. Interestingly, for the calcined sample treated at 773 K, the peak splitting of the CO vibrations is smaller than that (2179/2161 cm^{-1}) observed for the Pt/CeO_2 sample oxidized at 1073 K. This could be related to the relatively limited dispersion/ substitution of Pt in the sample oxidized at lower temperatures (773 K) and thus some ceria surfaces that are not in direct contact with Pt, as supported by the IR results for the re reduced samples discussed below.

When both samples were further reduced by heating in a hydrogen atmosphere at 530 K, the corresponding IR spectra change substantially (see Figure 4b). In both cases, intense CO bands below 2100 cm^{-1}, owing to the adsorption of CO on metallic Pt species, are observed. The reduction treatment of the oxidized (1073 K) Pt/CeO_2 yields a large number of CO bands, corresponding to CO species bound to various under coordinated Pt atop sites exposed by small clusters and CO adsorbed to bridge sites at the Pt (small clusters)−ceria interface.[18,51,52] In comparison, after reducing the calcined (773 K) sample, the SLIR spectrum is dominated by an intense CO band at 2069 cm^{-1} (Figure 4b), which is typical for CO adsorbed on high coordinated Pt atop sites of Pt NPs.[46−49] These findings reveal that the particles size of Pt species, generated under the same reduction conditions, varies

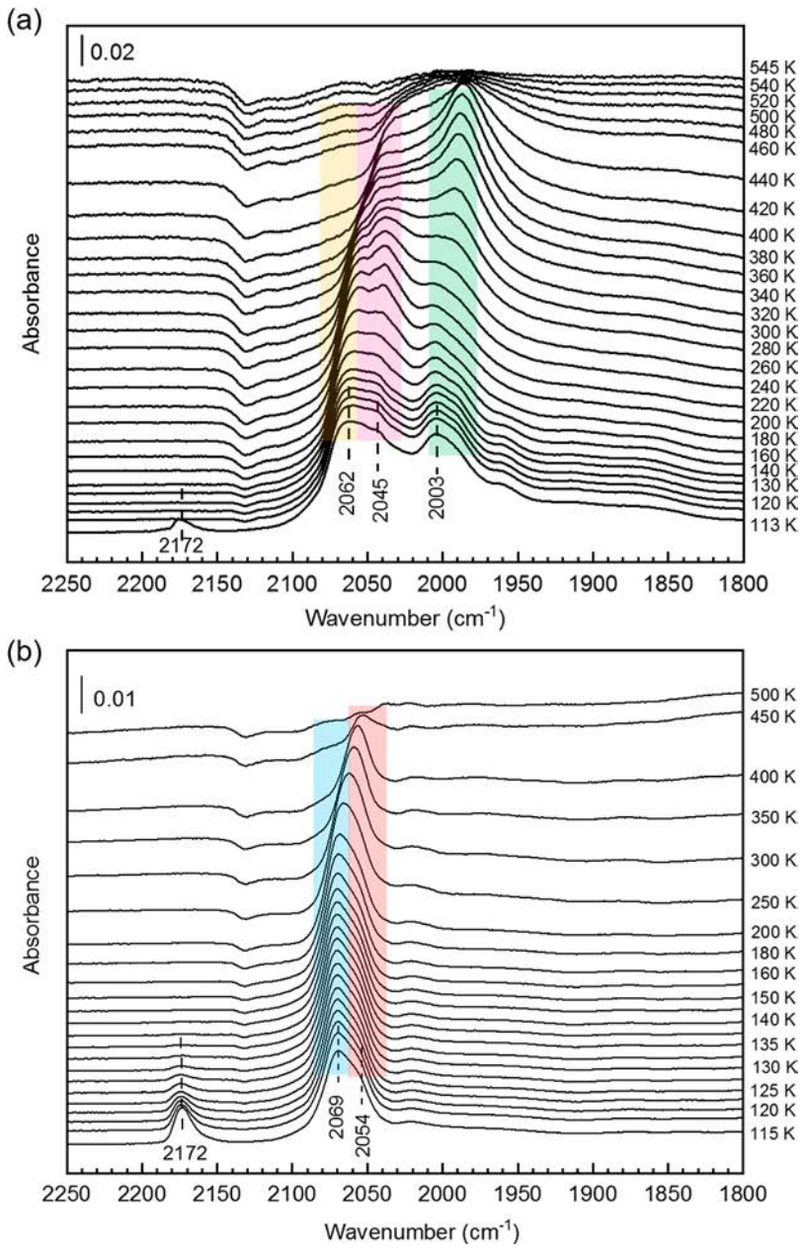

Figure 5. Temperature dependent CO SLIR spectra of Pt/CeO_2 catalysts obtained after reduction of (a) oxidized (1073 K) and (b) calcined (773 K) Pt/CeO_2 samples with H atoms at 530 K. The spectra were recorded after CO adsorption (0.01 mbar) at 113 and 115 K, respectively, followed by heating to indicated temperatures.

depending strongly on the initial dispersion states of Pt species formed under different oxidation conditions. It is expected that Pt shows a better dispersion in the oxidized Pt/CeO_2 due to the higher treatment temperature at 1073 K. Accordingly, the subsequent reduction in hydrogen at 530 K facilitates the formation of smaller Pt clusters on ceria surfaces. Hence, the Pt atoms must be better distributed over ceria and not migrate so easily to form larger clusters if oxidized at higher temperatures (1073 K vs 773 K).

Figure 5 presents the corresponding temperature dependent CO SLIR spectra of Pt/CeO_2 catalysts obtained by reducing the oxidized (1073 K) and calcined (773 K) Pt/CeO_2 samples with H atoms at 530 K. For the oxidized sample (Figure 5a), the peak at 2172 cm^{-1}, belonging to CO adsorbed on the CeO_2 support, vanishes at 125 K. However, the relative intensities of the CO bands at 2062, 2045, and 2003 cm^{-1} remain constant even upon heating to 200 K, indicating much stronger interactions between CO and metallic Pt species. As the temperature further increases, the peak at 2062 cm^{-1} gradually decreases in intensity and finally vanishes at 360 K. The peak at 2045 cm^{-1} disappears at a higher temperature (~500 K). The band at 2003 cm^{-1} shows a red shift with increasing temperature because of the decrease of CO coverage. The 2003 cm^{-1} band becomes the dominating one at temperature higher than 320 K and finally vanishes at 545 K. These results reveal that the CO species bound to Pt sites with lower coordination numbers are thermally more stable as they only vanish at higher temperatures. This finding is further supported by the results observed for the calcined (773 K) sample. As shown in Figure 5b, the predominant vibration at 2069 cm^{-1} (CO adsorbed to highly coordinated Pt atop sites) undergoes a red shift to about 2050 cm^{-1} with increasing

temperature and disappears after heating to 500 K, revealing a weaker interaction of CO molecules with Pt NPs.[53]

4. CONCLUSIONS

CO SLIR spectroscopy was used to characterize the dynamic structural evolution of Pt species on CeO_2 NPs under oxidative and reductive atmospheres. The IR results, together with XPS investigations, allow us to conclude that a substantial amount of Pt is substituted into the CeO_2 surface lattice after oxidation treatment at elevated temperatures, yielding positively charged, highly dispersed Pt species. The subsequent reduction in hydrogen leads to Pt surface segregation, yielding various metallic Pt species ranging from NPs to ultrafine clusters, as confirmed by the observation of characteristic CO IR bands. Our results reveal that higher oxidation temperatures (1073 K) promote the dispersion of Pt cations and, consequently, facilitate the formation of smaller metallic Pt clusters on CeO_2 along with the reduction at lower temperatures (530 K). The structural transformation of Pt species leads to strong changes in the electronic interactions between Pt and the ceria support, which directly affects the adsorption and the bond strength between the noble metal and adsorbates.

AUTHOR INFORMATION

Corresponding Authors

Yuemin Wang − *Institute of Functional Interfaces (IFG), Karlsruhe Institute of Technology (KIT), Eggenstein Leopoldshafen 76344, Germany;* orcid.org/0000 0002 9963 5473; Email: yuemin.wang@kit.edu

Christof Wöll − *Institute of Functional Interfaces (IFG), Karlsruhe Institute of Technology (KIT), Eggenstein Leopoldshafen 76344, Germany;* orcid.org/0000 0003 1078 3304; Email: christof.woell@kit.edu

Authors

Junjun Wang − *Engineering Research Center of Environmental Materials and Membrane Technology of Hubei Province, School of Materials Science and Engineering, Wuhan Institute of Technology, Wuhan 430074, China; Institute of Functional Interfaces (IFG), Karlsruhe Institute of Technology (KIT), Eggenstein Leopoldshafen 76344, Germany*

Eric Sauter − *Institute of Functional Interfaces (IFG), Karlsruhe Institute of Technology (KIT), Eggenstein Leopoldshafen 76344, Germany*

Alexei Nefedov − *Institute of Functional Interfaces (IFG), Karlsruhe Institute of Technology (KIT), Eggenstein Leopoldshafen 76344, Germany;* orcid.org/0000 0003 2771 6386

Stefan Heißler − *Institute of Functional Interfaces (IFG), Karlsruhe Institute of Technology (KIT), Eggenstein Leopoldshafen 76344, Germany*

Florian Maurer − *Institute for Chemical Technology and Polymer Chemistry (ITCP), Karlsruhe Institute of Technology (KIT), Karlsruhe 76131, Germany;* orcid.org/0000 0002 3307 4132

Maria Casapu − *Institute for Chemical Technology and Polymer Chemistry (ITCP), Karlsruhe Institute of Technology (KIT), Karlsruhe 76131, Germany;* orcid.org/0000 0002 8755 9856

Jan Dierk Grunwaldt − *Institute for Chemical Technology and Polymer Chemistry (ITCP), Karlsruhe Institute of Technology (KIT), Karlsruhe 76131, Germany; Institute of Catalysis Research and Technology (IKFT), Karlsruhe Institute of Technology (KIT), Eggenstein Leopoldshafen 76344, Germany;* orcid.org/0000 0003 3606 0956

Notes

The authors declare no competing financial interest.

ACKNOWLEDGMENTS

This work was funded by the Deutsche Forschungsgemeinschaft (DFG, German Research Foundation) — project ID 426888090 — SFB 1441 and the project 392178740. J.W. is grateful for PhD fellowships donated by the China Scholarship Council (CSC).

REFERENCES

(1) Fu, Q.; Saltsburg, H.; Flytzani Stephanopoulos, M. Active nonmetallic Au and Pt species on ceria based water gas shift catalysts. *Science* **2003**, *301*, 935−938.

(2) Goguet, A.; Meunier, F. C.; Tibiletti, D.; Breen, J. P.; Burch, R. Spectrokinetic investigation of reverse water gas shift reaction intermediates over a Pt/CeO_2 catalyst. *J. Phys. Chem. B* **2004**, *108*, 20240−20246.

(3) Luengnaruemitchai, A.; Osuwan, S.; Gulari, E. Comparative studies of low temperature water−gas shift reaction over Pt/CeO_2, Au/CeO_2, and Au/Fe_2O_3 catalysts. *Catal. Commun.* **2003**, *4*, 215−221.

(4) Jacobs, G.; Williams, L.; Graham, U.; Sparks, D.; Davis, B. H. Low temperature water gas shift: in situ DRIFTS− reaction study of a Pt/CeO_2 catalyst for fuel cell reformer applications. *J. Phys. Chem. B* **2003**, *107*, 10398−10404.

(5) Hardacre, C.; Ormerod, R. M.; Lambert, R. M. Platinum promoted catalysis by ceria: A study of carbon monoxide oxidation over Pt (111)/CeO_2. *J. Phys. Chem.* **1994**, *98*, 10901−10905.

(6) Gao, Y.; Wang, W.; Chang, S.; Huang, W. Morphology effect of CeO_2 support in the preparation, metal−support interaction, and catalytic performance of Pt/CeO_2 catalysts. *ChemCatChem* **2013**, *5*, 3610−3620.

(7) Nie, L.; Mei, D.; Xiong, H.; Peng, B.; Ren, Z.; Hernandez, X. I. P.; DeLaRiva, A.; Wang, M.; Engelhard, M. H.; Kovarik, L.; Datye, A. K.; Wang, Y. Activation of surface lattice oxygen in single atom Pt/CeO_2 for low temperature CO oxidation. *Science* **2017**, *358*, 1419−1423.

(8) Bera, P.; Gayen, A.; Hegde, M. S.; Lalla, N. P.; Spadaro, L.; Frusteri, F.; Arena, F. Promoting effect of CeO_2 in combustion synthesized Pt/CeO_2 catalyst for CO oxidation. *J. Phys. Chem. B* **2003**, *107*, 6122−6130.

(9) Chen, Y.; Li, H.; Zhao, W.; Zhang, W.; Li, J.; Li, W.; Zheng, X.; Yan, W.; Zhang, W.; Zhu, J.; et al. Optimizing reaction paths for methanol synthesis from CO_2 hydrogenation via metal ligand cooperativity. *Nat. Commun.* **2019**, *10*, 1885.

(10) Abid, M.; Touroude, R. Pt/CeO_2 catalysts in selective hydrogenation of crotonaldehyde: high performance of chlorine free catalysts. *Catal. Lett.* **2000**, *69*, 139−144.

(11) Abid, M.; Ehret, G.; Touroude, R. Pt/CeO_2 catalysts: correlation between nanostructural properties and catalytic behaviour

in selective hydrogenation of crotonaldehyde. *Appl. Catal. A* **2001**, *217*, 219−229.
(12) Kalakkad, D. S.; Datye, A. K.; Robota, H. J. Pt CeO_2 contact and its effect on CO hydrogenation selectivity. *J. Catal.* **1994**, *148*, 729−736.
(13) Liao, L.; Mai, H. X.; Yuan, Q.; Lu, H. B.; Li, J. C.; Liu, C.; Yan, C. H.; Shen, Z. X.; Yu, T. Single CeO_2 nanowire gas sensor supported with Pt nanocrystals: gas sensitivity, surface bond states, and chemical mechanism. *J. Phys. Chem. C* **2008**, *112*, 9061−9065.
(14) Golunski, S. E.; Hatcher, H. A.; Rajaram, R. R.; Truex, T. J. Origins of low temperature three way activity in Pt/CeO_2. *Appl. Catal., B* **1995**, *5*, 367−376.
(15) Pantu, P.; Gavalas, G. R. Methane partial oxidation on Pt/CeO_2 and Pt/Al_2O_3 catalysts. *Appl. Catal. A* **2002**, *223*, 253−260.
(16) Gänzler, A. M.; Casapu, M.; Vernoux, P.; Loridant, S.; Cadete Santos Aires, F. J.; Epicier, T.; Betz, B.; Hoyer, R.; Grunwaldt, J. D. Tuning the structure of platinum particles on ceria in situ for enhancing the catalytic performance of exhaust gas catalysts. *Angew. Chem., Int. Ed.* **2017**, *56*, 13078−13082.
(17) Bell, A. T. The impact of nanoscience on heterogeneous catalysis. *Science* **2003**, *299*, 1688−1691.
(18) Qiao, B.; Wang, A.; Yang, X.; Allard, L. F.; Jiang, Z.; Cui, Y.; Liu, J.; Li, J.; Zhang, T. Single atom catalysis of CO oxidation using Pt_1/FeO_x. *Nat. Chem.* **2011**, *3*, 634−641.
(19) Liu, L.; Corma, A. Metal Catalysts for Heterogeneous Catalysis: From single atoms to nanoclusters and nanoparticles. *Chem. Rev.* **2018**, *118*, 4981−5079.
(20) Lykhach, Y.; Kozlov, S. M.; Skála, T.; Tovt, A.; Stetsovych, V.; Tsud, N.; Dvořák, F.; Johánek, V.; Neitzel, A.; Mysliveček, J.; et al. Counting electrons on supported nanoparticles. *Nat. Mater.* **2016**, *15*, 284−288.
(21) Peter, M.; Flores Camacho, J. M.; Adamovski, S.; Ono, L. K.; Dostert, K. H.; O'Brien, C. P.; Roldan Cuenya, B.; Schauermann, S.; Freund, H. J. Trends in the binding strength of surface species on nanoparticles: how does the adsorption energy scale with the particle size? *Angew. Chem., Int. Ed.* **2013**, *52*, 5175−5179.
(22) Nagai, Y.; Dohmae, K.; Ikeda, Y.; Takagi, N.; Tanabe, T.; Hara, N.; Guilera, G.; Pascarelli, S.; Newton, M. A.; Kuno, O.; et al. In situ redispersion of platinum autoexhaust catalysts: an on line approach to increasing catalyst lifetimes? *Angew. Chem., Int. Ed.* **2008**, *47*, 9303−9306.
(23) Hinokuma, S.; Fujii, H.; Okamoto, M.; Ikeue, K.; Machida, M. Metallic Pd nanoparticles formed by Pd O Ce interaction: a reason for sintering induced activation for CO oxidation. *Chem. Mater.* **2010**, *22*, 6183−6190.
(24) Gänzler, A. M.; Casapu, M.; Maurer, F.; Störmer, H.; Gerthsen, D.; Ferré, G.; Vernoux, P.; Bornmann, B.; Frahm, R.; Murzin, V.; et al. Tuning the Pt/CeO_2 interface by in situ variation of the Pt particle size. *ACS Catal.* **2018**, *8*, 4800−4811.
(25) Maurer, F.; Jelic, J.; Wang, J.; Gänzler, A.; Dolcet, P.; Wöll, C.; Wang, Y.; Studt, F.; Casapu, M.; Grunwaldt, J. D. Tracking the formation, fate and consequence for catalytic activity of Pt single sites on CeO_2. *Nat. Catal.* **2020**, *3*, 824−833.
(26) Wöll, C. Structure and chemical properties of oxide nanoparticles determined by surface ligand IR spectroscopy. *ACS Catal.* **2020**, *10*, 168−176.
(27) Wang, Y.; Wöll, C. IR spectroscopic investigations of chemical and photochemical reactions on metal oxides: bridging the materials gap. *Chem. Soc. Rev.* **2017**, *46*, 1875−1932.
(28) Chen, A.; Yu, X.; Zhou, Y.; Miao, S.; Li, Y.; Kuld, S.; Sehested, J.; Liu, J.; Aoki, T.; Hong, S.; et al. Structure of the catalytically active copper−ceria interfacial perimeter. *Nat. Catal.* **2019**, *2*, 334−341.
(29) Yang, C.; Capdevila Cortada, M.; Dong, C.; Zhou, Y.; Wang, J.; Yu, X.; Nefedov, A.; Heißler, S.; López, N.; Shen, W.; et al. Surface refaceting mechanism on cubic ceria. *J. Phys. Chem. Lett.* **2020**, *11*, 7925−7931.
(30) Kleist, W.; Grunwaldt, J. D. High output catalyst development in heterogeneous gas phase catalysis. In *Modern applications of high throughput R&D in heterogeneous catalysis*; Hagemeyer, A., Volpe, A. F., Jr., Eds.; Bentham Science Publisher, 2014; p 357.
(31) Wang, Y.; Glenz, A.; Muhler, M.; Wöll, C. New dual purpose ultrahigh vacuum infrared spectroscopy apparatus optimized for grazing incidence reflection as well as for transmission geometries. *Rev. Sci. Instrum.* **2009**, *80*, 113108.
(32) Doniach, S.; Sunjic, M. Many electron singularity in X Ray photo emission and X Ray line spectra from metals. *J. Phys. C: Solid State Phys.* **1970**, *3*, 285−291.
(33) Dvořák, F.; Camellone, M. F.; Tovt, A.; Tran, N. D.; Negreiros, F. R.; Vorokhta, M.; Skála, T.; Matolínová, I.; Mysliveček, J.; Matolín, V. Creating single atom Pt ceria catalysts by surface step decoration. *Nat. Commun.* **2016**, *7*, 10801.
(34) Bera, P.; Patil, K. C.; Jayaram, V.; Subbanna, G. N.; Hegde, M. S. Ionic dispersion of Pt and Pd on CeO_2 by combustion method: Effect of metal−ceria interaction on catalytic activities for NO reduction and CO and hydrocarbon oxidation. *J. Catal.* **2000**, *196*, 293−301.
(35) Sharma, S.; Hegde, M. S. Pt metal CeO_2 interaction: Direct observation of redox coupling between $Pt^0/Pt^{2+}/Pt^{4+}$ and Ce^{4+}/Ce^{3+} states in $Ce_{0.98}Pt_{0.02}O_{2-\delta}$ catalyst by a combined electrochemical and X ray photoelectron spectroscopy study. *J. Chem. Phys.* **2009**, *130*, 114706.
(36) Kottwitz, M.; Li, Y.; Palomino, R. M.; Liu, Z.; Wang, G.; Wu, Q.; Huang, J.; Timoshenko, J.; Senanayake, S. D.; Balasubramanian, M.; Lu, D.; Nuzzo, R. G.; Frenkel, A. I. Local structure and electronic state of atomically dispersed Pt supported on nanosized CeO_2. *ACS Catal.* **2019**, *9*, 8738−8748.
(37) Pereira Hernández, X. I.; DeLaRiva, A.; Muravev, V.; Kunwar, D.; Xiong, H.; Sudduth, B.; Engelhard, M.; Kovarik, L.; Hensen, E. J. M.; Wang, Y.; Datye, A. K. Tuning Pt CeO_2 interactions by high temperature vapor phase synthesis for improved reducibility of lattice oxygen. *Nat. Commun.* **2019**, *10*, 1358.
(38) Wang, H.; Liu, J. X.; Allard, L. F.; Lee, S.; Liu, J.; Li, H.; Wang, J.; Wang, J.; Oh, S. H.; Li, W. Surpassing the single atom catalytic activity limit through paired Pt O Pt ensemble built from isolated Pt_1 atoms. *Nat. Commun.* **2019**, *10*, 3808.
(39) Burroughs, P.; Hamnett, A.; Orchard, A. F.; Thornton, G. Satellite structure in the X ray photoelectron spectra of some binary and mixed oxides of lanthanum and cerium. *J. Chem. Soc., Dalton Trans.* **1976**, *17*, 1686−1698.
(40) Yang, C.; Yu, X.; Heißler, S.; Nefedov, A.; Colussi, S.; Llorca, J.; Trovarelli, A.; Wang, Y.; Wöll, C. Surface faceting and reconstruction of ceria nanoparticles. *Angew. Chem., Int. Ed.* **2017**, *56*, 375−379.
(41) Liu, H. H.; Wang, Y.; Jia, A. P.; Wang, S. Y.; Luo, M. F.; Lu, J. Q. Oxygen vacancy promoted CO oxidation over Pt/CeO_2 catalysts: A reaction at Pt−CeO_2 interface. *Appl. Surf. Sci.* **2014**, *314*, 725−734.
(42) Machocki, A.; Ioannides, T.; Stasinska, B.; Gac, W.; Avgouropoulos, G.; Delimaris, D.; Grzegorczyk, W.; Pasieczna, S. Manganese−lanthanum oxides modified with silver for the catalytic combustion of methane. *J. Catal.* **2004**, *227*, 282−296.
(43) Holgado, J. P.; Munuera, G.; Espinós, J. P.; González Elipe, A. R. XPS study of oxidation processes of CeO_x defective layers. *Appl. Surf. Sci.* **2000**, *158*, 164−171.
(44) Wang, G. D.; Kong, D. D.; Pan, Y. H.; Pan, H. B.; Zhu, J. F. Low energy Ar ion bombardment effects on the CeO_2 surface. *Appl. Surf. Sci.* **2012**, *258*, 2057−2061.
(45) Stetsovych, V.; Pagliuca, F.; Dvořák, F.; Duchoň, T.; Vorokhta, M.; Aulická, M.; Lachnitt, J.; Schernich, S.; Matolínová, I.; Veltruská, K.; et al. Epitaxial cubic Ce_2O_3 films via Ce−CeO_2 interfacial reaction. *J. Phys. Chem. Lett.* **2013**, *4*, 866−871.
(46) Takeguchi, T.; Manabe, S.; Kikuchi, R.; Eguchi, K.; Kanazawa, T.; Matsumoto, S.; Ueda, W. Determination of dispersion of precious metals on CeO_2 containing supports. *Appl. Catal., A* **2005**, *293*, 91−96.
(47) Gao, H.; Xu, W.; He, H.; Shi, X.; Zhang, X.; Tanaka, K. I. DRIFTS investigation and DFT calculation of the adsorption of CO on Pt/TiO_2, Pt/CeO_2 and $FeO_x/Pt/CeO_2$. *Spectrochim. Acta, Part A* **2008**, *71*, 1193−1198.

(48) Sakamoto, Y.; Higuchi, K.; Takahashi, N.; Yokota, K.; Doi, H.; Sugiura, M. Effect of the addition of Fe on catalytic activities of Pt/Fe/γ Al_2O_3 catalyst. *Appl. Catal., B* **1999**, *23*, 159−167.
(49) Raskó, J. CO induced surface structural changes of Pt on oxide supported Pt catalysts studied by DRIFTS. *J. Catal.* **2003**, *217*, 478−486.
(50) Ding, K.; Gulec, A.; Johnson, A. M.; Schweitzer, N. M.; Stucky, G. D.; Marks, L. D.; Stair, P. C. Identification of active sites in CO oxidation and water gas shift over supported Pt catalysts. *Science* **2015**, *350*, 189−192.
(51) Bazin, P.; Saur, O.; Lavalley, J. C.; Daturi, M.; Blanchard, G. FT IR study of CO adsorption on Pt/CeO_2: characterisation and structural rearrangement of small Pt particles. *Phys. Chem. Chem. Phys.* **2005**, *7*, 187−194.
(52) Aleksandrov, H. A.; Neyman, K. M.; Hadjiivanov, K. I.; Vayssilov, G. N. Can the state of platinum species be unambiguously determined by the stretching frequency of an adsorbed CO probe molecule? *Phys. Chem. Chem. Phys.* **2016**, *18*, 22108−22121.
(53) Casapu, M.; Fischer, A.; Gänzler, A. M.; Popescu, R.; Crone, M.; Gerthsen, D.; Türk, M.; Grunwaldt, J. D. Origin of the normal and inverse hysteresis behavior during CO oxidation over Pt/Al_2O_3. *ACS Catal.* **2017**, *7*, 343−355.

Karlsruher Institut für Technologie

OPEN ACCESS

Repository KITopen

Dies ist ein Postprint/begutachtetes Manuskript.

Empfohlene Zitierung:

Wang, J.; Sauter, E.; Nefedov, A.; Heißler, S.; Maurer, F.; Casapu, M.; Grunwaldt, J.-D.; Wang, Y.; Wöll, C.
Dynamic Structural Evolution of Ceria-Supported Pt Particles: A Thorough Spectroscopic Study
2022. The Journal of Physical Chemistry C.
doi:10.5445/IR/1000146585

Zitierung der Originalveröffentlichung:

Wang, J.; Sauter, E.; Nefedov, A.; Heißler, S.; Maurer, F.; Casapu, M.; Grunwaldt, J.-D.; Wang, Y.; Wöll, C.
Dynamic Structural Evolution of Ceria-Supported Pt Particles: A Thorough Spectroscopic Study
2022. The Journal of Physical Chemistry C.
doi:10.1021/acs.jpcc.2c02420

Lizenzinformationen: KITopen-Lizenz